Canadian Mineralogist
Vol. 26, pp. 467-486 (1988)

GEOLOGICAL MAPPING OF THE EAST PACIFIC RISE AXIS (10°19′ – 11°53′N) USING THE ARGO AND ANGUS IMAGING SYSTEMS

ARGO-RISE GROUP[1]

ABSTRACT

The Acoustically Navigated Geological Underwater Survey (ANGUS) and Argo systems were used to map the Neovolcanic Zone of a segment of the East Pacific Rise from just north of the Clipperton Fracture Zone at 10°19′N to 11°53′N, including the overlapping spreading centers and overlap basin from 11°39′N to 11°51′N. The Neovolcanic Zone on the ridge segment east of the overlap basin is dominated by at least two generations of relatively recent volcanic sheet-flow units, with associated collapse structures and hydrothermal deposits, superimposed on an older sediment-laden pillow terrane. Recent volcanic activity along the ridge north of the Clipperton Fracture Zone and west of the overlap basin is restricted to a narrow zone on two axial topographic highs centered at 10°55′N and 11°26′N, extending as far south as 10°37′N and as far north as 11°51′N. North of about 10°52′N, this recent volcanic activity is restricted to an axial graben 10–100 m wide and 20 m deep. South of 10°50′N to about 10°38′N, recent volcanic activity occurred along a constructional high. The floor of the overlap basin consists mainly of old sedimented pillows. On the eastern ridge of the overlapping spreading centers, hydrothermal vents occur within collapse structures. On the ridge segment north of the Clipperton Fracture Zone and west of the overlap basin, hydrothermal vents occur along fault complexes that flank the ridge crest and axial graben. These observations support the concept that magmatic activity along spreading centers is episodic and that such activity is not continuous throughout the ridge segments at any given time. We propose that the magmatism follows a cyclical pattern, progressing from initial pillow-lava emplacement, to extrusion of sheet flows, to a waning phase of pillow extrusion, and finally to pelagic sedimentation.

Keywords: geology, maps, volcanic sheet flows, pillow lavas, cyclical magmatism, hydrothermal vents, Neovolcanic Zone, East Pacific Rise.

SOMMAIRE

Les systèmes de télédétection ANGUS (Acoustically Navigated Geological Underwater Survey) et Argo ont été utilisés pour cartographier la zone néovolcanique d'un segment de la dorsale Est-Pacifique de 10°19′N, immédiatement au nord de la zone de fractures de Clipperton, jusqu'à 11°53′N. Sont inclus dans ce secteur les centres de séparation qui se chevauchent, et le bassin de chevauchement de 11°39′N à 11°51′N. La zone néovolcanique le long de la crête à l'est du bassin de chevauchement montre surtout deux générations d'épanchements volcaniques relativement récents, en forme de feuille, avec structures d'effondrement et manifestations hydrothermales associées, sur un socle de laves en coussins recouvert de sédiments. L'activité volcanique récente, le long d'une crête au nord de la zone de Clipperton et à l'ouest du bassin de chevauchement, est localisée dans une zone étroite sur deux accidents topographiques axiaux situés à 10°55′N et 11°26′N, et s'étendant vers le sud jusqu'à 10°37′N et vers le nord jusqu'à 11°51′N. Au nord de 10°52′N, environ, l'activité récente est limitée à un graben axial de 10 à 100 m de large et profond de 20 m. Au sud de 10°50′N, jusqu'à 10°38′N environ, les manifestations récentes ont contribué à former un édifice. Le plancher du bassin de chevauchement est surtout parsemé de coussins anciens sédimentés. Sur la crête orientale de la zone de chevauchement des centres de séparation, les évents hydrothermaux occupent les structures d'effondrement. Le long de la section de la dorsale au nord de la zone de Clipperton et à l'ouest du bassin de chevauchement, les évents hydrothermaux se trouvent le long de systèmes de failles qui longent la crête de la dorsale et le graben axial. Ces observations étayent l'hypothèse d'une activité magmatique épisodique le long des dorsales, activité qui n'est pas continue le long d'un segment. L'activité magmatique suivrait une évolution cyclique: mise en place de laves en coussins, suivie d'extrusion de coulées en feuilles, et enfin formation de lave en coussins en stade terminal. Le tout est suivi de sédimentation pélagique.

(Traduit par la Rédaction)

Mots-clés: géologie, cartes, coulées en feuille, laves en coussins, magmatisme cyclique, évents hydrothermaux, zone néovolcanique, dorsale Est-Pacifique.

INTRODUCTION

Studies of the Neovolcanic Zones of mid-ocean ridges have given rise to a debate about the volcanotectonic processes that are active at spreading centers. To understand better this complex geologic setting, the crest of the East Pacific Rise (EPR) from 10°19′N (just north of the Clipperton Fracture Zone) to 11°53′N (Fig. 1) was investigated using the Acoustically Navigated Geological Underwater Survey (ANGUS) and Argo systems (Ballard 1980, Harris & Ballard 1986). In this report, we describe the results of the geologic mapping of the region.

Studies of the crestal zone of mid-ocean ridges have shown that segments between transform faults

[1]R.D. Ballard, E. Uchupi, Woods Hole Oceanographic Institution, Woods Hole, Massachusetts 02543; D.K. Blackman, Brown University, Providence, Rhode Island 02912; J.L. Cheminee, J. Francheteau, Institut de Physique du Globe de Paris, France; R. Hékinian, IFREMER, Centre de Brest, B.P. 337-2973, Brest Cedex, France; W.C. Schwab, U.S. Geological Survey, Woods Hole, Massachusetts 02543; H. Sigurdsson, University of Rhode Island, Kingston, Rhode Island 02881.

or overlapping spreading centers (OSCs) display a single regional topographic high, and that water depth increases in the direction of the transform faults and OSCs (Lonsdale 1977, 1983, 1985a, 1985b, Ballard & Francheteau 1982, 1983, Macdonald 1982, Francheteau & Ballard 1983, Macdonald & Fox 1983, Macdonald *et al.* 1984). Along the Mid-Atlantic Ridge, where the transform faults are closely spaced (40–50 km), the amplitude of this along-axis relief can be as high as 2,500 m. On the EPR, ridge segments between large transform faults are up to 350 km in length, and those between small offset transform zones (including OSCs) are about 60–70 km long (Schouten *et al.* 1985). As the depth variation along EPR segments is only 200–300 m, the along-strike topographic gradients are much gentler.

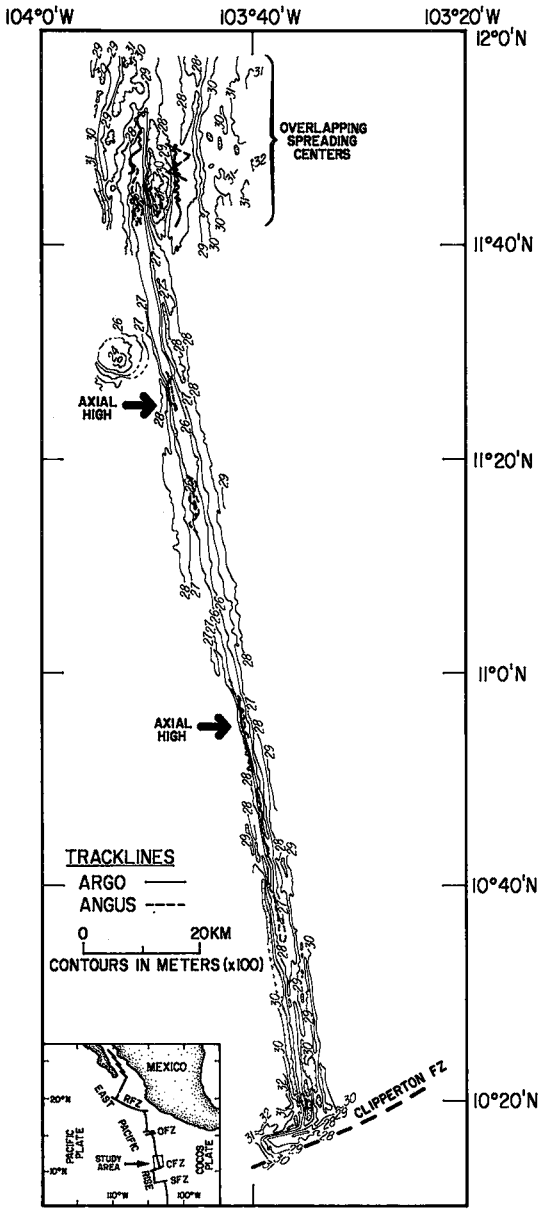

FIG. 1. Location map of the study area showing the ANGUS and Argo tracklines. RFZ Rivera Fracture Zone; OFZ Orozco Fracture Zone; CFZ Clipperton Fracture Zone; SFZ Siqueiros Fracture Zone.

Ridge-crest topographic highs are the sites of active hydrothermal processes. They are characterized by abundant volcanic sheet flows or fluid lavas (equivalent to subaerial surface-fed pahoehoe flows; Ballard *et al.* 1979) and by a regional lack of fissures and faults (Ballard *et al.* 1983). Pillow lavas (analogous to subaerial tube-fed pahoehoe flows; Ballard *et al.* 1979), fissures, and faults are more abundant along strike, away from the regional topographic highs and in the direction of the transform faults (Ballard & Francheteau 1983). To account for these along-strike variations in tectonic style, Francheteau & Ballard (1983) proposed that each mid-ocean ridge segment is underlain by a magma chamber and that this chamber has its maximum development beneath the topographic high. This hypothesis is in agreement with the suggestion that the elevation of the Neovolcanic Zone of mid-ocean ridges is directly related to the height reached by upwelling magma along the ridge axis. This elevation is a function of the rate of magma supply relative to spreading rate (Deffeyes 1970, Sleep 1969, 1975, Vogt 1976, Anderson & Noltimier 1973, Crane 1985, Macdonald *et al.* 1984, 1986, Detrick *et al.* 1987).

Since geologic studies of the Neovolcanic Zone of the EPR have concentrated on topographic highs that are typically marked by recent volcanism and hydrothermal activity, there is a need to extend detailed studies along the strike of the ridge. In this paper, we present the results of geological mapping based on still photography and video data along 90 km of the crest of the EPR, north of the Clipperton Fracture Zone (CFZ) (Fig. 1). Results from dredging programs over the same region are described elsewhere (Thompson *et al.* 1985, Langmuir *et al.* 1986). Our observations show that recent volcanic sheet flows, possibly less than 100 years old, are superimposed on an older sediment-laden pillow terrane. The spatial and temporal relationships between the pillow flows and the younger volcanic flow units indicate that magmatic activity is episodic and discontinuous along the Neovolcanic Zone at any given time, and suggest that volcanic activity along the crest of the EPR is due to the expansion and contraction of a magma chamber away from a fixed injection point which is located at the regional topographic highs. These interpretations are in general agreement with those of Francheteau & Ballard (1983) and Macdonald *et al.* (1984, 1986).

METHODS

Assessment of the seafloor topography and surficial distribution of volcanic rock types along the crest of the EPR from 10°19′N to 11°53′N was obtained from 50,200 ANGUS bottom photographs and 120 km of Argo video, supplemented with Seabeam bathymetry (Macdonald *et al.* 1984). The ANGUS data were collected aboard the RV *MELVILLE*, Protea Expedition, Leg 9 in the summer of 1984, and the Argo data aboard the same vessel in December 1985 during the Ice Expedition, Leg 1. The Argo and ANGUS vehicles were navigated using bottom-moored acoustic transponders. The locations of the transponders were obtained using shipboard Global Positioning System (GPS) and transit satellite navigation systems.

ANGUS is a color camera system designed to work in extremely rugged terranes (Ballard 1980). Photos were taken every 20 seconds at tow speeds of 0.8–2.0 km/hr, resulting in as much as 50% overlap. ANGUS was normally towed at an elevation of 10 m above the seafloor; the photographic coverage at that altitude was 192 m^2 for a camera with a 16-mm lens, and 15 m^2 for one with a 50-mm lens. Argo is a deeply towed vehicle that operates at heights of 10–40 m above the seafloor (Harris & Ballard 1986). The Argo sled carries three Silicon Intensified Target (SIT) video cameras, with a 12-mm down-looking lens, a 24-mm foward-looking lens, and a down looking 24–80 mm zoom lens. A thermistor was added to the Argo and ANGUS systems for this study in order to identify temperature anomalies related to hydrothermal activity.

A series of geologic maps and cross-sections (Figs. 2–11) was compiled based on the combined ANGUS and Argo data sets. The Neovolcanic Zone defined by these maps is offset 100–200 m west of the location determined from the bathymetric analyses of Macdonald *et al.* (1984). Because the Argo and ANGUS systems were navigated using bottom transponders, GPS, and satellite navigation to an accuracy of 5 m, the Seabeam bathymetric maps (Macdonald *et al.* 1984) were modified using the better navigated Argo and ANGUS bathymetry, and adjusted to the geologic maps.

GEOMORPHOLOGIC SETTING

The ridge crest of the EPR between the Clipperton and Orozco fracture zones consists of a chain of subparallel topographic highs 2–10 km wide, 200–400 m high, and 40–140 km long (Klitgord & Mammerickx 1982, Macdonald *et al.* 1984). In the study area, the Neovolcanic Zone straddling the crest of the EPR is less than 1 km wide. Along strike, the zone north of the CFZ displays a progressive shallowing to a topographic high at 10°55′N with a minimum water depth of 2,540 m (Figs. 6–9), from where the zone gradually deepens northward to the small topographic low at 11°15′N (Fig. 5). From this low, the Neovolcanic Zone rises gently to a second topographic high at 11°26′N and a water depth of 2,510 m (Fig 4), then again deepens to the OSCs at 11°45′N (Fig. 3). The OSCs at 11°45′N curve slightly away from each other before they overlap and then curve back toward each other in the overlap region, enclosing a depression with an elliptical shape that is aligned subparallel to the spreading center. The OSCs that surround the overlap basin are offset by about 8 km.

The Neovolcanic Zone also displays considerable topographic variation in cross-section. From south of 10°45′N to the CFZ, the Neovolcanic zone has a triangular cross-section (Figs. 7–9). According to Macdonald *et al.* (1984), the summit graben atop the crest of the EPR is nearly continuous from 10°N to 13°N. However, features less than 100 m wide and 5 m deep may not be resolvable from the Seabeam bathymetry and SeaMARC I sonographs used by Macdonald *et al.* (1984). The ANGUS and Argo data show that a well-developed summit graben is limited to a region from 10°52′N north to at least 11°28′N (Figs. 4–6). In this region, the Neovolcanic Zone has a dome-like cross-section; its summit graben has a relief of 20 m and a width of less than 200 m (Francheteau & Ballard 1983, Hékinian *et al.* 1985b). The configuration of the Neovolcanic Zone south of approximately 10°49′N is a miniature ridge and trough terrane with no singular summit graben developed.

The individual ridges of the OSCs (Fig. 3) are asymmetrical in cross-section; the steeper sides face the overlap basin. The flanks of the individual ridges are fragmented by closely spaced (1–2 km) normal fault scarps 5–10 km long (Lonsdale 1977, Macdonald 1982). These scarps produce an undulating horst and graben topography with a wavelength of 2–4 km and an amplitude of 50–100 m (Macdonald *et al.* 1984). On the eastern ridge of the OSCs (Fig. 10), cross-sections display morphologies ranging from a broad low with an irregular floor, to a broad dome, to a collapse plateau (Fig. 11).

VOLCANIC FLOW UNITS

The volcanic terranes noted on the Argo and ANGUS video and photo data were classified into three units on the basis of flow morphology, degree of freshness, relative amount of pelagic sediment cover, and location of the unit with respect to the EPR axis (Table 1). The youngest unit (Unit I) straddles the Neovolcanic Zone and is represented by glassy lobate to smooth sheet flows (Fig. 12A). These relatively fluid flows grade laterally onto older lobate flows (Unit II) or merge with sediment-laden pillow flows (Unit III). The contacts between the Unit I and

II flows are gradational, whereas the contacts between these units and Unit III flows are irregular. Unit I lobate flows cascade over individual pillows or meander along depressions between pillows (Fig. 13A). In some areas, Unit III pillow terrane occurs several meters above the surface of the Unit I glassy lobate flows. In Unit I terrane, the ratio of lobate to pillow flows is >10:1.

The lobate flow surface in the Unit I terrane has collapsed leaving 5–15 m deep depressions in some places (Fig. 12B, C). These collapse structures have highly irregular outlines (in plan view), some display overhangs or arches, and most display more than one collapse level. Collapse levels are thought to reflect inflation and deflation cycles of the underlying magma chamber, and are expressed as vertical fluctuations in the lava-pond surface (Ballard *et al.* 1979, Francheteau *et al.* 1979). At the edge of the collapse structures, rubble aprons formed from glassy fragments of the collapsed roof are commonly found in association with arches and pillars. However, the rubble diminishes toward the center of many of the collapse areas, and is replaced by various types of Unit I sheet flows: smooth, ropy, hackly, and jumbled.

Unit II flows are lobate flows that are thought to be of intermediate age (partly glassy to dull with minor sediment cover; Fig. 12D). The ratio of lobate to pillow flows in Unit II terrane ranges from 5:1 to 3:1. Unit II flows also display collapse structures, some of which are invaded by Unit I glassy flows. Unit I flows were also found in fissures (gja), within the lava pond floors of Unit II terrane.

Unit III, the most extensive unit mapped, and thought to be the oldest, consists of pillow lavas and lobate flows with a sediment cover of more than 15% (Fig. 13A). In places this sediment cover masks the volcanic terrane (Fig. 13B).

Evidence of hydrothermal activity was found in Unit I and II terranes and, in some places, along fractures in Unit III terrane. This evidence includes hydrothermal precipitates recognized by their texture or yellow staining, temperature anomalies, shimmering water, and associated fauna such as brachyuran crabs, ophiuroids, clams, mussels, and serpulid worms (Fig. 14). With a few exceptions, active vents were found only in Unit I terrane. These active vents appear to be of the low-temperature Galapagos type, with hot water emanating from between lobes of basalt. Serpulid worms were found only at two locations during this investigation, 10°44.6′N (Fig. 7) and 11°46.65′N (Fig. 3); clams and mussels were found only at the 10°44.6′N vent.

The percentage of sediment cover can be used to estimate the relative age of the underlying basalt (van Andel & Ballard 1979, Ballard *et al.* 1981, 1982). We used visual observations and sampling results from submersible studies on the EPR near 12°53′N

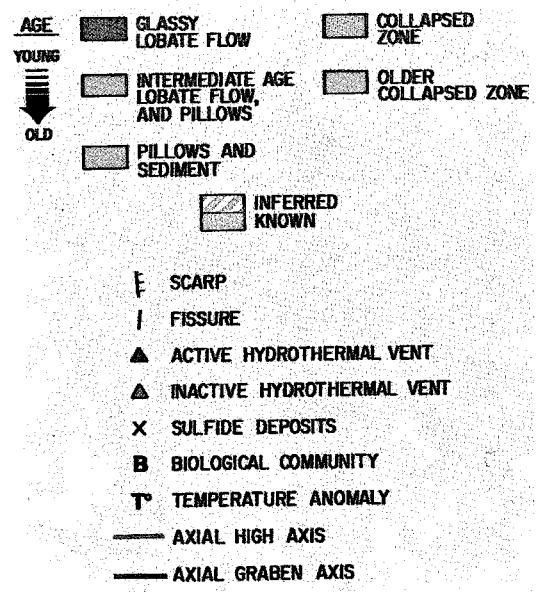

FIG. 2. Symbols used in Figures 3 to 10.

(CYATHERM, unpubl. results, Hékinian *et al.* 1985a) in an attempt to quantify this dating procedure. These studies near 12°53′N suggest that the thickness of sediment on relatively young crust (<200,000 years old) is roughly proportional to the percentage of sediment cover. If this observation is applicable to our study area, then sediment thickness on Unit III terrane would be at least 10 cm. Assuming a linear sedimentation rate of 1.7 cm/1000 years (Rosendahl *et al.* 1980), Unit III flows should be older than 6,000 years. Unit II flows, with less than 5% sediment cover, should be less than 2000 years old, and the glassy flows of Unit I are less than 100 years old. In support of this young age estimate for Unit I flows, a hydrothermal field in the axial graben (Unit I terrane) to the north of our study area has been estimated to have formed within the last 100 years on the basis of growth rates of sulfide stacks (Hékinian *et al.* 1985b), an age later corroborated by radio-isotope dating of the stacks (Lalou *et al.* 1985). Although these semi-quantitative age estimates are based on submersible studies approximately 100 km north of our study area, and factors such as variable microtopographic relief and redistribution of sediment by bottom currents introduce errors, these approximate ages are all that can be used until an accurate technique of dating relatively young mid-ocean ridge basalts is developed.

AREAS STUDIED BY FINE-SCALE IMAGING

Overlapping spreading centers (11°45′N)

Recent volcanic and hydrothermal activity is restricted to the eastern ridge of the 11°45′N OSCs (Fig.

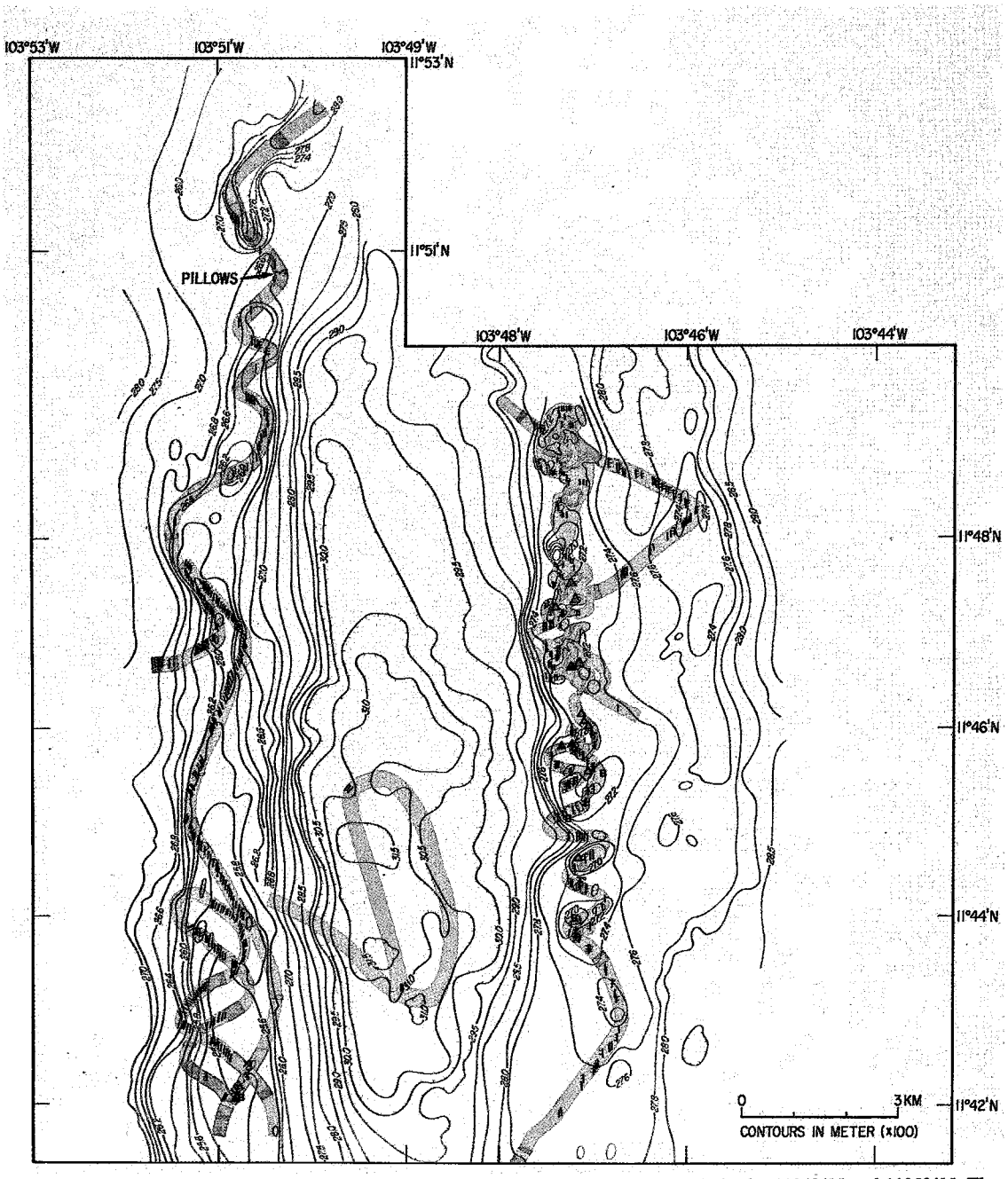

FIG. 3. Interpreted surficial geology of the overlapping spreading centers between latitudes 11°42′N and 11°53′N. The bathymetry in this and Figures 4 to 10 was modified from Macdonald *et al.* (1984).

3). Glassy lobate flows of Unit I and associated collapse structures represent more than 60% of the area surveyed on the eastern ridge. At 11°48′N, Unit I flows are separated by a volcanic cone, 100 m high, south of which they gradually diminish in extent, whereas Units II and III flows increase in extent. Limited video coverage over this volcanic cone suggest that it is constructed of Unit III terrane. Unit I flows on the eastern ridge segment of the 11°45′N OSCs apparently were emplaced within collapse structures that developed on Unit II flows, and on sags and downdrop blocks on Unit III terrane (Figs.

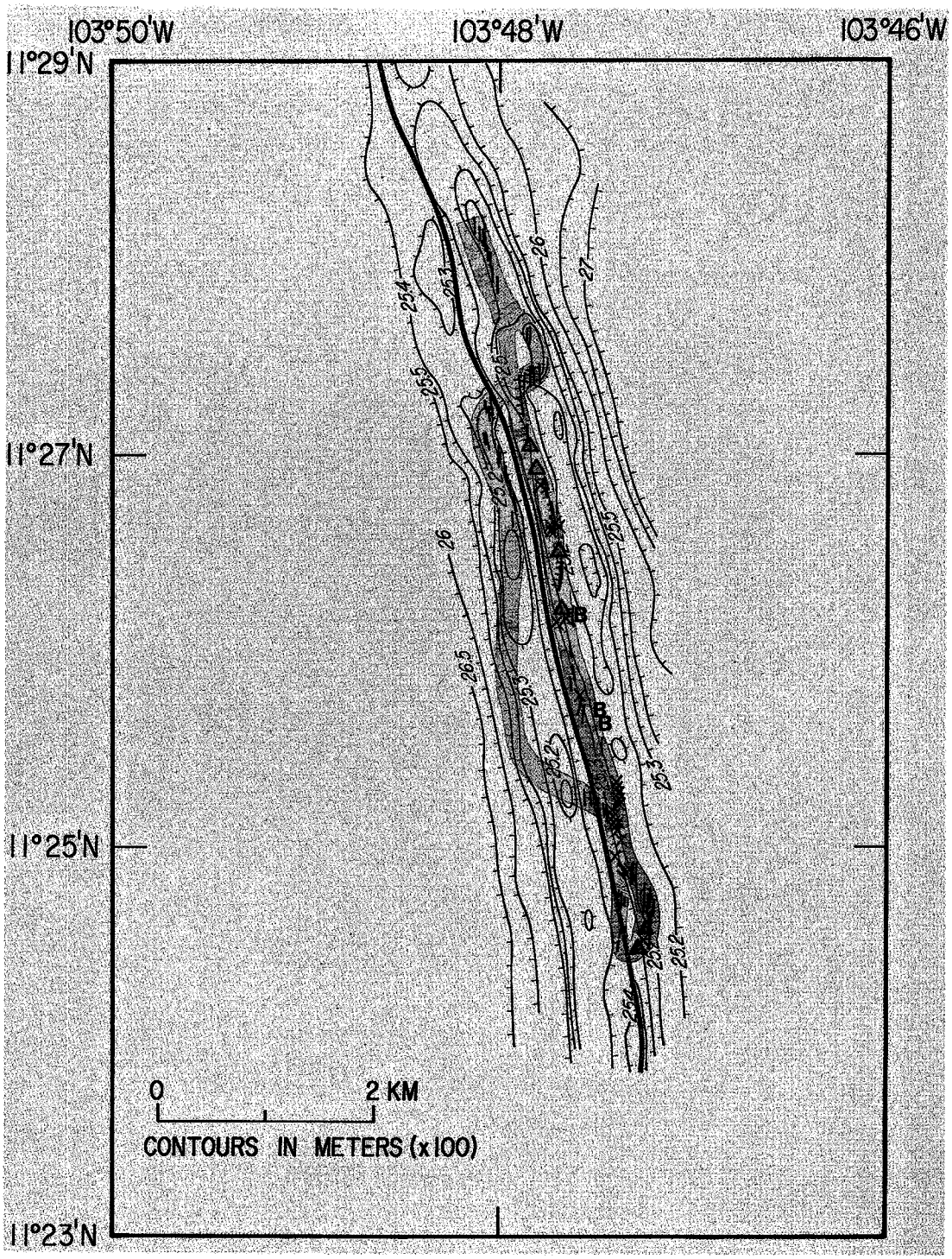

FIG. 4. Interpreted surficial geology of a segment of the EPR between latitudes 11°23′N and 11°29′N.

10, 11). Five large collapse structures occur within the Unit I terrane on the eastern ridge segment, two north and three south of the volcanic cone at 11°48′ N. These structures, which are elongate in a north–south direction, are 100–300 m wide, 200–400 m long, and 5–15 m deep. At least two phases of extru-

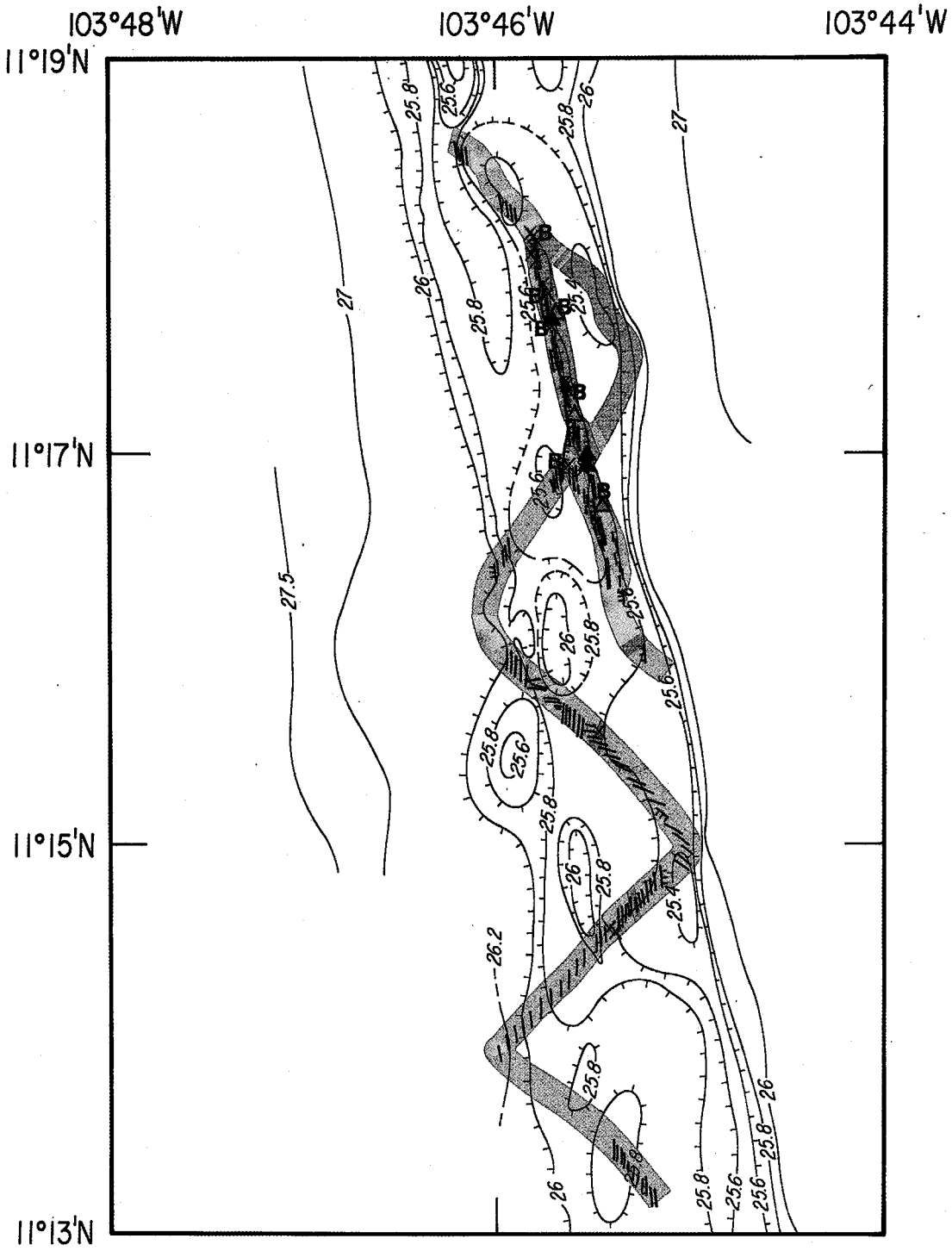

FIG. 5. Interpreted surficial geology of a segment of the EPR between latitudes 11°13′N and 11°19′N.

sion and collapse of Unit I sheet flows were identified. Collapse of these lava ponds is thought to have been caused by lateral flow of the magma away from the crestal zone. Fissures are common on the lava-pond floors and also within 50 m of the lava-pond edges. These latter fissures are invaded by Unit I

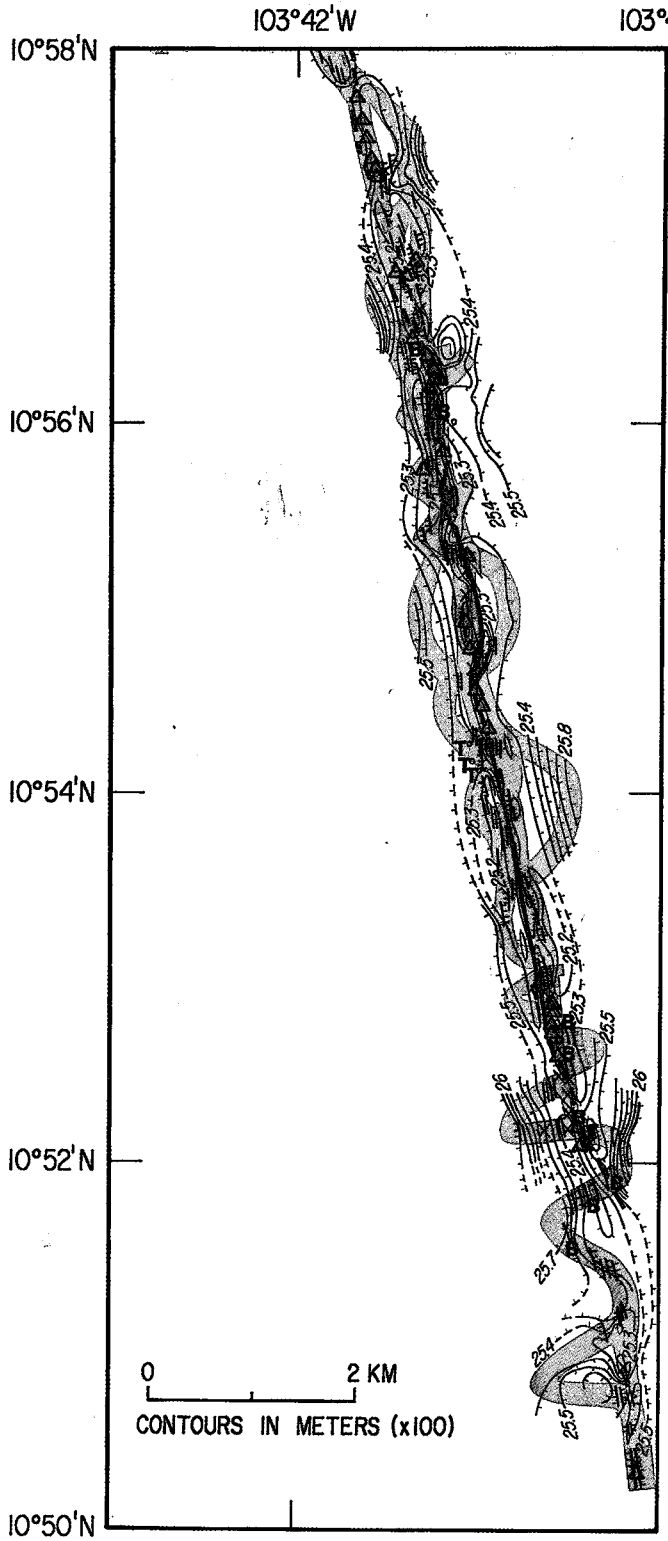

FIG. 6. Interpreted surficial geology of a segment of the EPR between latitudes 10°50′N and 10°58′N.

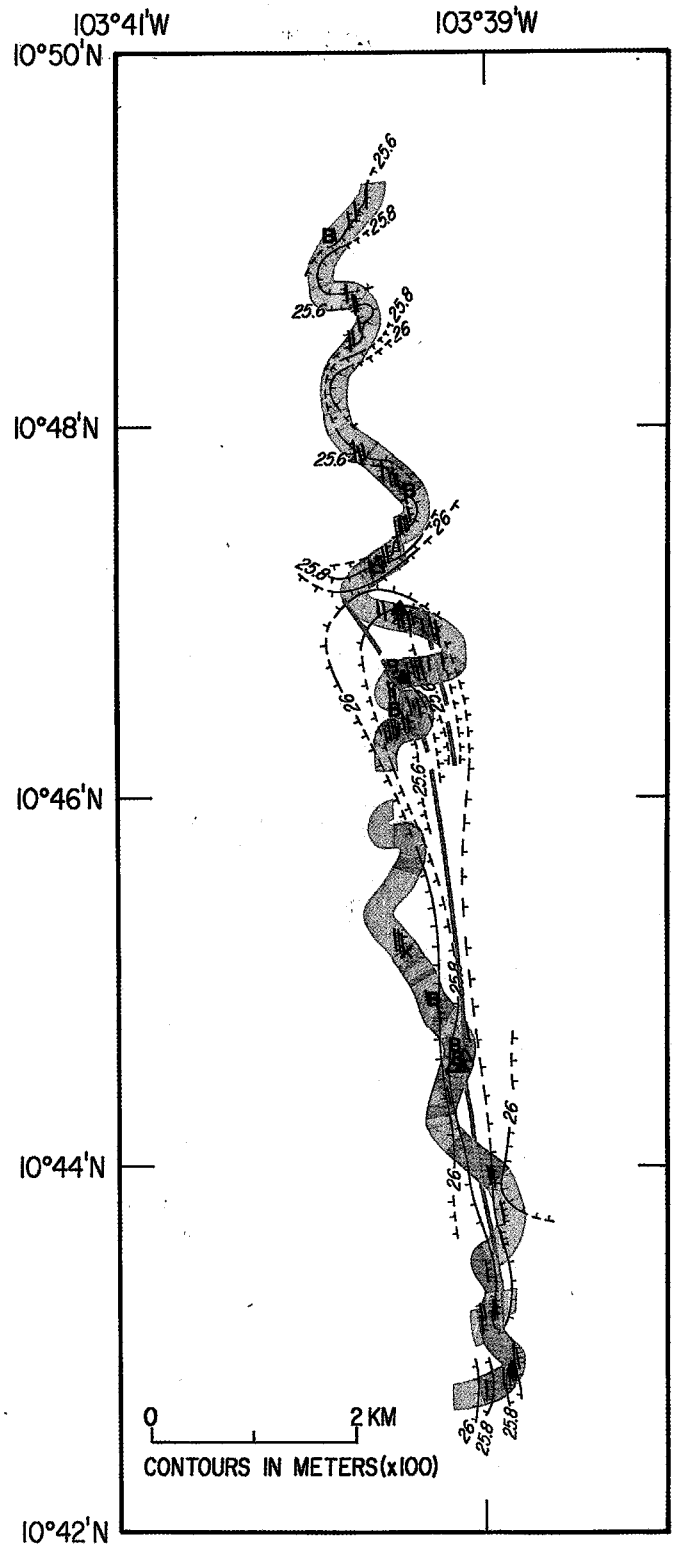

FIG. 7. Interpreted surficial geology of a segment of the EPR between latitudes 10°42′N and 10°50′N.

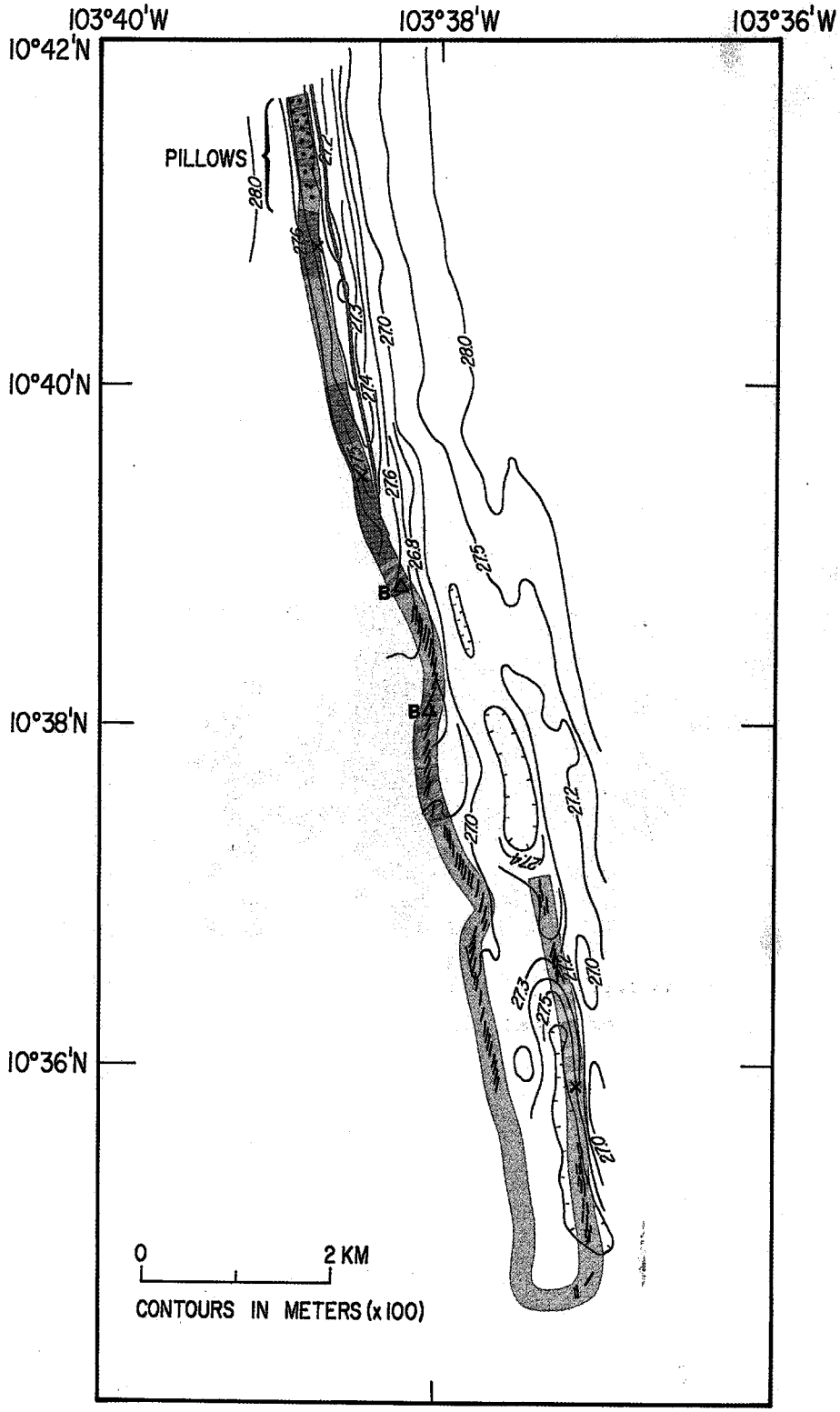

FIG. 8. Interpreted surficial geology of a segment of the EPR between latitudes 10°35′N and 10°42′N.

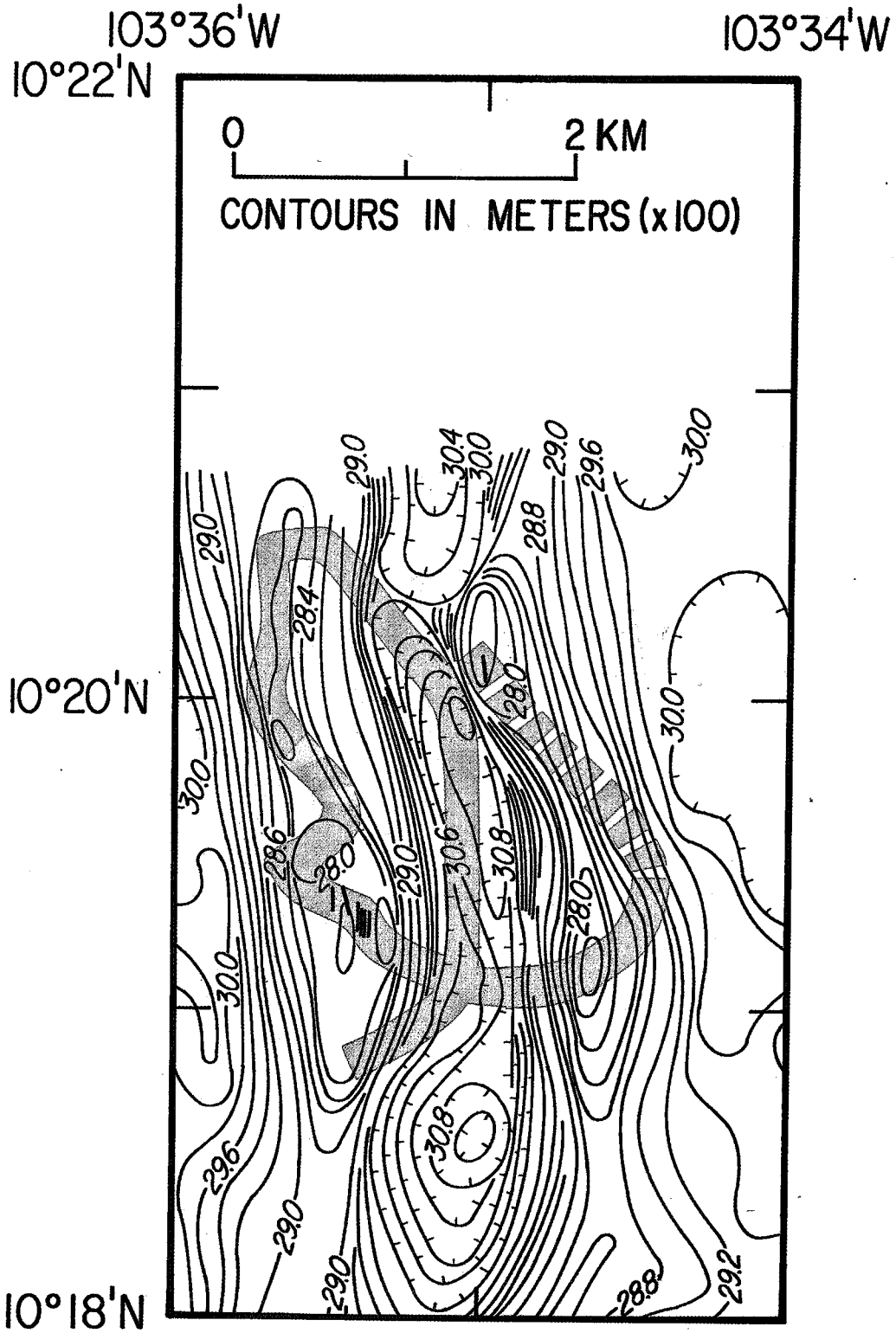

FIG. 9. Interpreted surficial geology of a segment of the EPR between latitudes 10°18′N and 10°22′N.

FIG. 10. Interpreted surficial geology of the eastern ridge of the overlapping spreading center shown in Figure 3.

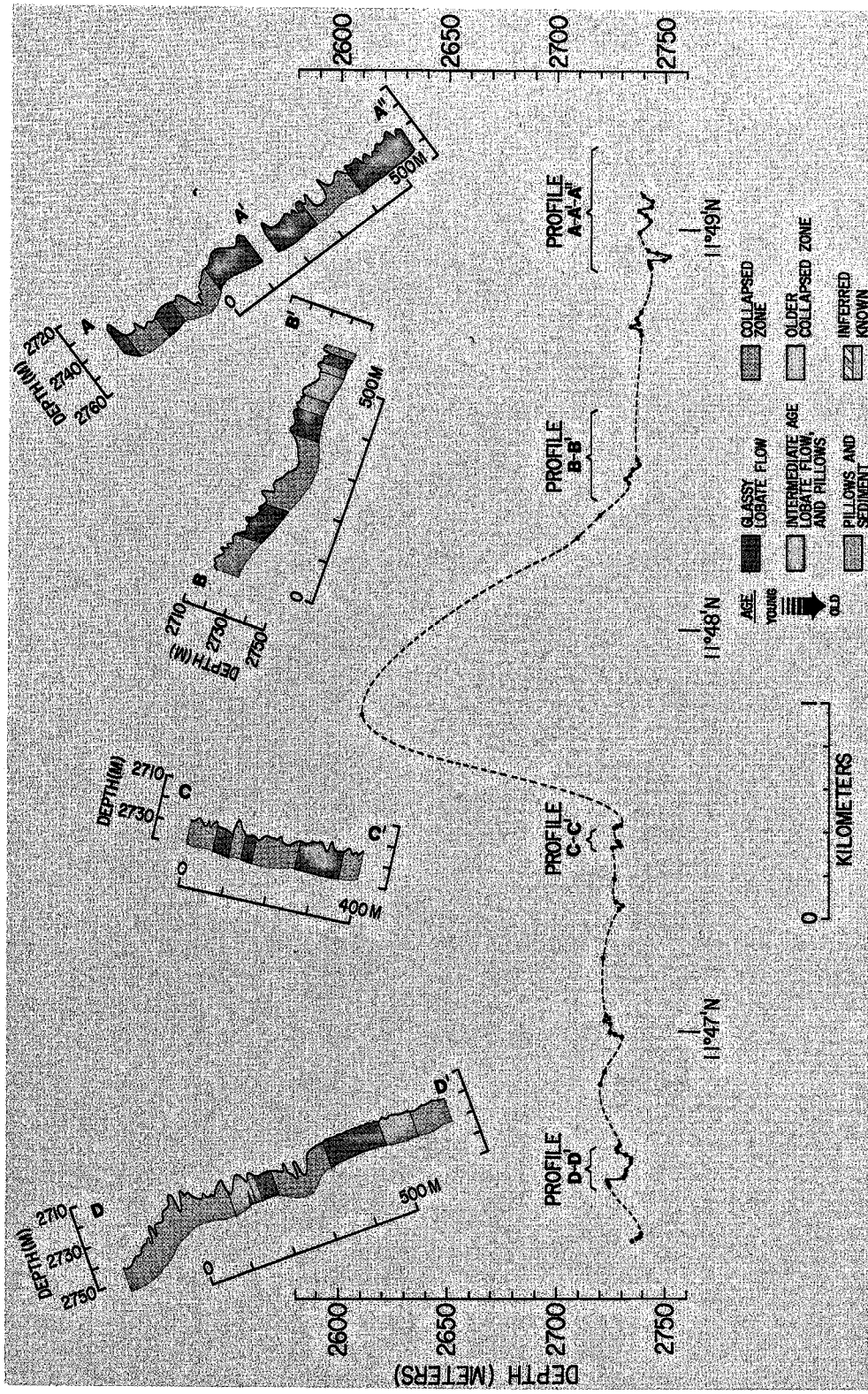

FIG. 11. A series of geologic sections showing the surficial geology over the eastern ridge of the overlapping spreading center shown in Figure 3. The locations of these sections are shown on Figure 10.

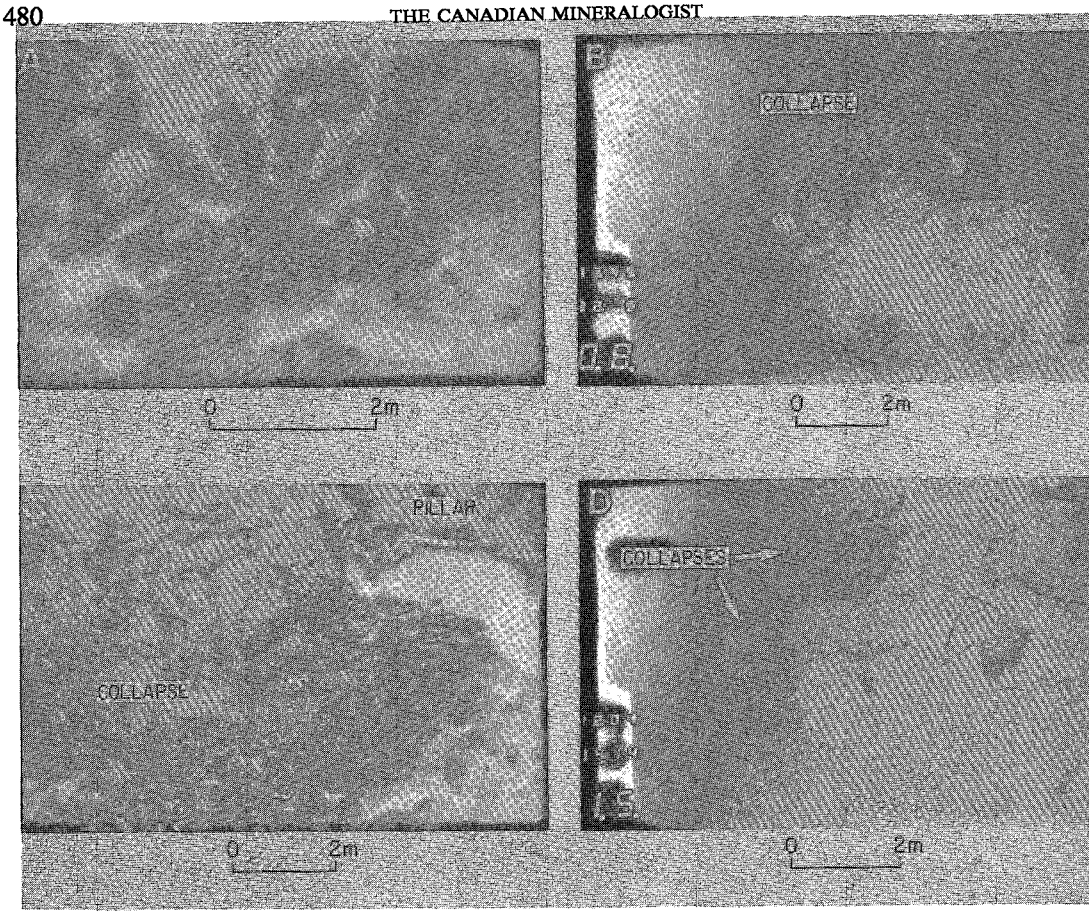

FIG. 12. 35-mm Argo photographs of (A) a Unit I glassy lobate basalt flow, (B) the edge of a large collapse structure in Unit I terrane, (C) the floor of a collapse structure in Unit I terrane, and (D) small collapse structures in Unit II terrane.

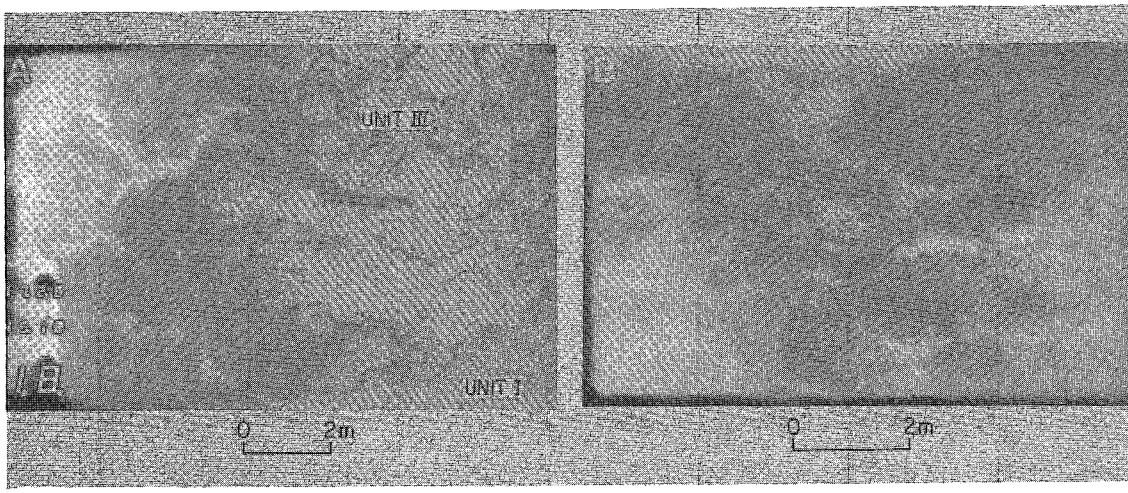

FIG. 13. (A) 35-mm ANGUS photograph of a Unit I glassy lobate basalt flow emplaced over a Unit III pillow basalt terrane. (B) 35-mm Argo photograph of Unit III pillow basalt terrane with an extensive sediment cover.

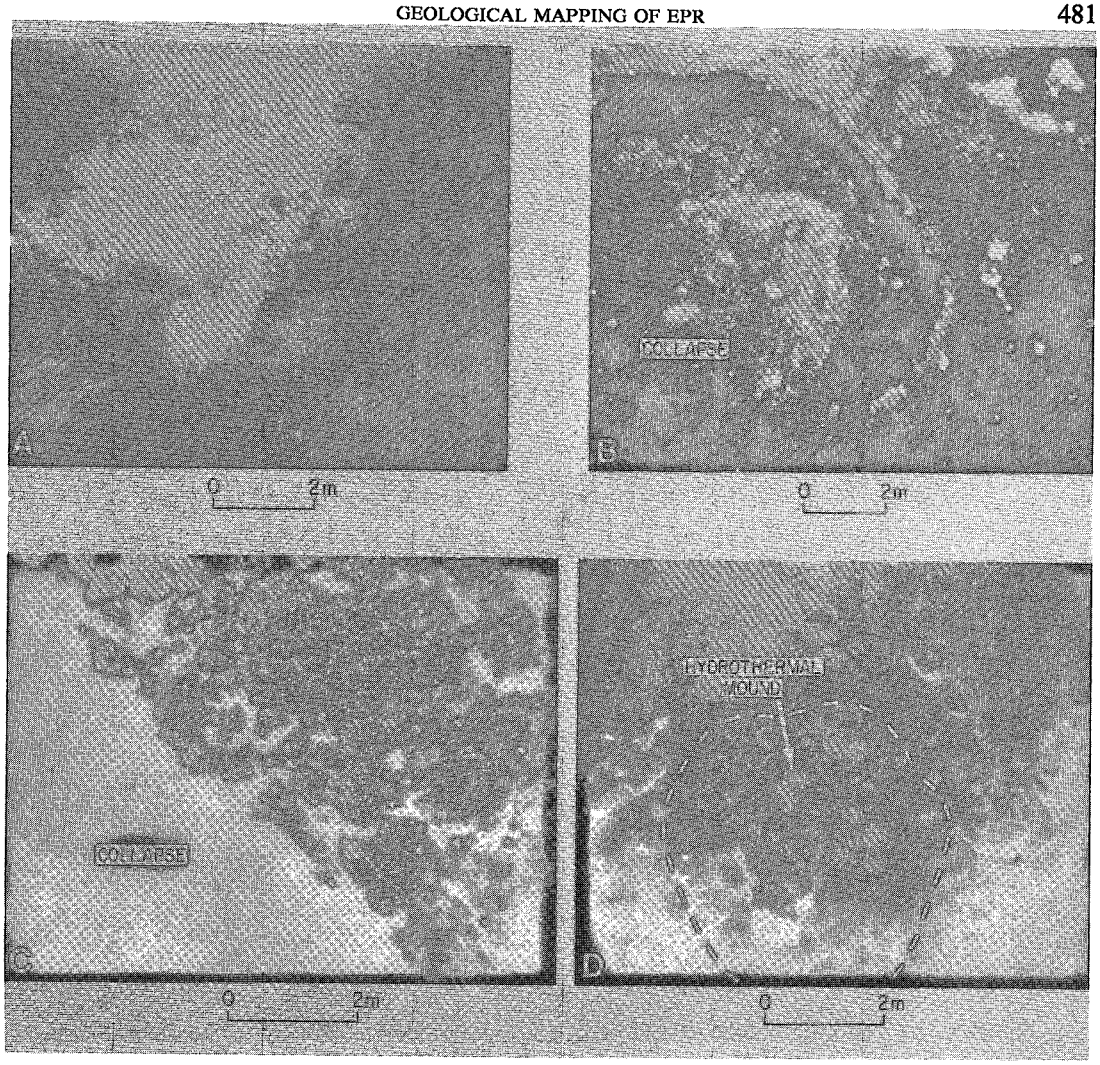

FIG. 14. 35-mm Argo photographs of (A) an active (smoking) hydrothermal vent in Unit I terrane, (B) an area of hydrothermal venting in a collapse structure in Unit I terrane with clams and mussels, (C) an area of hydrothermal venting in Unit I terrane showing a large group of brachyuran crabs, and (D) an inactive hydrothermal vent and sulfide deposits distinguished by a bright yellow stain on Unit II lobate basalt flows.

flows, suggesting that the fissures are pathways of lava drainage from, or lava supply to the floors of the lava ponds. In some areas, the roofs of the lava ponds collapsed into underlying fluid lavas; fragments now form slabs in the solidified matrix of the flows. In these areas, Unit I flows have a lumpy texture, apparently the result of partial remelting of roof fragments (Fig. 12C). Associated with the collapses south of the volcanic cone are at least five inactive hydrothermal vents and their fragmented sulfide deposits. Profiles along the strike of the EPR axis (Fig. 11), across the large collapses, show gentle slope gradients. North of the volcanic cone at 11°48′N, the floors of the collapses dip northward with a declivity of about 0.25°, whereas south of the volcanic cone, the declivity of the floors of the collapses between 11°46.5′N and 11°47.5′N is toward the north. South of 11°46.5′N, the floors deepen toward the south.

Within the 4-km-wide overlap basin at 11°45′N, Unit III flows are heavily sedimented (Fig. 3). In the center of the basin, at water depths in excess of 3,100 m, the volcanic terrane is no longer discernible. The extent of the sediment cover is thought to be evidence that this volcanic terrane is older than the Unit III terrane found on the flank and crest of the eastern ridge segment, although it is possible that some sediment has collected preferentially in the topographic low. Based on limited ANGUS coverage (Fig. 3), we found no evidence of recent tectonic or volcanic

TABLE 1. CLASSIFICATION AND RELATIVE AGE ESTIMATES OF VOLCANIC TERRANES ALONG THE EAST PACIFIC RISE AXIS, 10°15'-11°50'N.

CLASSIFICATION	MORPHOLOGY	FLOW TYPES	VISUAL OBSERVATIONS	DISTANCE FROM EPR AXIS (m)	ESTIMATED AGE (yr)
Unit I: Young	Lava pond	Flat, ropy & hackly	Entirely glassy	0-300	less than 100(?)
"	Shallow collapse pits	Lobate & pillow	"	"	"
Unit II: Intermediate Age	Lava pond	Flat, ropy & hackly	Partly glassy	0-500	100-500
"	Shallow collapse pits	Lobate & pillow	"	"	"
"	Lava pond & collapse pits	Flat, ropy & hackly, lobate & pillow	Dull with sediment dusting	0-700	500-1750
Unit III: Old Age	Collapse pit	Lobate & pillow	Dull with sediment cover (5-15%)	0-1000	<2,000-6,000
"	Bulbous/ tubular	Pillow & lobate	Dull with sediment cover (15-25%)	0-1500	6,000-10,000
"	Partly buried	Pillow	Sediment cover >25%	>300	>10,000

activity in the overlap basin as suggested by Lonsdale (1985a).

The crest of the western ridge of the 11°45'N OSCs is covered mainly by pillows and sediment of Unit III, along with scattered patches of Unit II lobate flows (Fig. 3). Immediately south of the OSCs, at 11°42'N on the crest of the ridge, active hydrothermal vents occur in association with a highly fractured plateau-like terrain consisting of Unit II sedimented, lobate to smooth flows.

Regional topographic highs

The segment of the EPR between 10°52'N and 11°28'N is cut at its summit by a discontinuous axial graben 10–100 m wide and 10–30 m deep (Figs. 4–6). The walls of the graben generally consist of normal-fault blocks of Unit III flows. The outward-facing slopes of the regional highs are of constructional origin, consisting of old pillow terrane cut by fissures. Between latitudes 11°24'N and 11°28'N, the narrow graben is bordered on the east by a ridge which shoals to a water depth of 2,510 m (Fig. 4). Along this ridge are a line of extensive hydrothermal deposits and inactive vents (see also Hékinian *et al.* 1985b). The floor of the axial graben between 11°24'N and 11°28'N is covered by Unit I lobate flows near the center of the low, and by talus at the base of the marginal scarps. Farther south (Fig. 5), an axial graben, 50 m wide and 10–20m deep, was mapped from 11°16'N to 11°18'N. The floor of the graben is covered by Unit I and II flows and its eastern side is marked by active hydrothermal vents. The broad eastern marginal scarp also is also covered by Unit I lobate flows.

From 10°52'N to 10°58'N (Fig. 6), the axial graben contains Unit I flows and collapses, and Unit II lobate flows. Along the crests of the marginal scarps are stacks and mounds of hydrothermal deposits. A hydrothermal stack at 10°55.75'N, active during the Protea Expedition in the summer of 1984, was inactive during the Ice Expedition in December, 1985. Submersible surveys of the 10°55.75'N hydrothermal area by the D.S.R.V. ALVIN (May, 1984) indicated that the main sulfide zone was located on a fissure system, but that the hydrothermal activity was patchy. Two main sulfide mounds in this area are reported to contain about 200 tonnes of hydrosulfides (McConachy *et al.* 1986). Near 10°55.7'N and 10°56.4'N, depressions in the Unit II terrane are partly invaded by Unit I lobate flows and hydrothermal deposits; the latter are particularly abundant on the highs at 10°52.2'N, 10°55.7'N and 10°56'N (Fig. 6).

Regional topographic lows

The EPR segment between the CFZ at 10°17'N and the regional topographic high at 10°55'N is a regional low (water depth 3,090 m at 10°19'N); the ridge segment has a triangular cross-section and lacks a summit graben south of about 10°49'N (Figs. 7–9). East of the crest of the EPR, an elongate topographic depression, extending south of 10°38'N to the CFZ (Figs. 8, 9), is devoid of Unit I or II flows but contains pillows, lobate flows, volcanic rubble, and collapse structures laden with sediment. This terrane, together with the overlap basin at 11°45'N, appears to be the oldest segment of seafloor encountered during this investigation (based on the amount of sediment cover). A ridge flanking the eastern side of this elongate topographic depression is not a volcanic constructional high, but is a horst in Unit III terrane (Fig. 9). The ridge bounding the western side is a volcanic constructional high composed of Unit III flows (Figs. 8, 9). Some of these pillows have a relatively fresh appearance whereas others are dull and partly covered by sediment, suggesting that at least two generations of pillows make up this western ridge.

South of 10°42'N (Figs. 8, 9), Unit I flows occur in patches at 10°38'N, 10°39'N, and 10°41'N. At 10°41.5'N, glassy pillow flows were observed (Fig. 8); this site is one of two where this flow type occurs in the study area. The rest of the ridge segment south of 10°42'N is mantled by Unit III pillow terrane.

The crest of the unrifted segment of the EPR between 10°49'N and 10°43'N is a site of Unit I lobate flows (Fig. 7). These flows are glassier or fresher than the Unit I flows on the regional topographic highs at 10°55'N (Fig. 6) and 11°26'N (Fig. 4). Three active hydrothermal vents were observed in this Unit I terrane (Fig. 7). Based on a model of symmetrical, exponential decreases in the number of brachyuran crabs with distance from the vent centers, van Dover *et al.* (1987) predicted the location of 3

additional vents, presumably skirted by the Argo vehicle. The observed vents appear to be of the low-temperature, Galapagos type, with hot water emanating between lobes of lava. However, the zone of venting at 10°44.6′N covered an area of about 15,000 m^2, the largest single area of hydrothermal activity found during this investigation. This is one of two zones that contained serpulid worms, and is the only area where clams and mussels were observed.

Discussion

Studies of the crest of mid-ocean ridges suggest that the elevation of the ridge axis is a direct measure of the height reached by upwelling magma along the axis, a function of the magma budget (Francheteau & Ballard 1983, Macdonald *et al.* 1984, Detrick *et al.* 1987). Francheteau & Ballard (1983) predicted that a regional topographic high above the crest of a magma chamber should be mantled by sheet flows, with thermal effects at a maximum. Away from the high, along the axial strike, there should be a decrease in the ratio of lobate to pillow flows and in hydrothermal activity (Ballard *et al.* 1979). Our observations along the crest of the EPR from the CFZ to the western ridge of the 11°45′N, OSCs in general display these features, although the lobate flows are superimposed on an older pillow terrane (Table 1). Thus, an initial phase of magmatic activity that emplaced pillow flows (>6,000 years ago) was followed by a period of volcanic quiescence (sedimentation), then a second phase of activity (about 500 years ago) that emplaced sheet flows atop the pillows. Hydrothermal activity seems to be associated only with this second phase of magmatic activity; however, older hydrothermal sulfide deposits and staining could easily be masked by the accumulation of pelagic sediment.

The second phase of magmatic activity (Units I and II) along the ridge segment north of the CFZ to the western ridge of the 11°45′N, OSCs was not limited to the topographic highs but extended discontinuously 65 km south of the high centered at 10°55′N (Fig. 9) and 48 km north of the 11°26′N high (Fig. 3). Similarly, evidence of hydrothermal activity extends 32 km south of the 10°55′N high (Fig. 8) and 30 km north of the 11°26′N high (Fig. 3). The most recent magmatic activity (Unit I) extended 33 km south of the 10°55′N high (Fig. 8) and 46 km north of the 11°26′N high (Fig. 3), where a glassy pillow flow was observed (11°51′N).

Seismic-refraction studies along the EPR had previously suggested the possible absence of a magma chamber near 11°19′N (Bratt & Solomon 1984). Multichannel seismic-reflection profiles indicate that an axial magma chamber reflection is absent along the EPR between the CFZ and 11°N, but north of 11°N a narrow (<4–6 km wide) axial magma chamber reflection is generally continuous for a distance of 77 km along-axis to about 11°42′N (Detrick *et al.* 1987). These observations suggest that the magma chamber is small or partly solidified on this ridge segment (Detrick *et al.* 1987). With the exception of a glassy pillow flow at 11°51′N and an active hydrothermal vent at 11°42′N, the lack of recent volcanic activity (Unit I) on the western ridge of the 11°45′N OSCs (Fig. 3) correlates well with the reported absence of an axial magma chamber north of 11°42′N. Although seismic-reflection profiles suggest that the axial magma chamber is not developed between the CFZ and 11°N (Detrick *et al.* 1987), the presence of Unit I flows as far south as 10°38′N (Fig. 8) suggests that a magmatic source (or sources) is present. Recent results from ophiolite studies in Oman (A. Nicolas, oral comm., 1987) suggest that major, along-strike transport of magma from a central magma chamber can be expected in a setting like the EPR. Thus, the recent volcanic activity along the ridge axis indicates the presence of a magma chamber, but not necessarily beneath that part of the ridge axis.

Macdonald *et al.* (1988) suggest that the two regional topographic highs separated by a low at 11°15′N are the result of the collision of two propagating magma chambers. However, seismic-reflection profiles (Detrick *et al.* 1987) show no pronounced change in the configuration of the roof of the magma chamber beneath this topographic low. The topographic low instead may be the result of the contraction of a single magma chamber which underlies both the topographic highs and the intervening low. This scenario predicts that the morphology of the ridge is due to the expansion and depletion of the magma chamber, similar to the model proposed by Macdonald *et al.* (1986). When the chamber expands, sheet flows and hydrothermal activity characterize much of the ridge. As the magmatic activity wanes, emplacement of lava becomes more discontinuous along the ridge, and sheet flows give way to pillow lavas, a relation analogous to that between surface-fed and tube-fed pahoehoe flows in subaerial eruptions (Ballard *et al.* 1979). With continued depletion of the magma chamber, even pillow emplacement ceases, and pelagic sedimentation predominates. In time, another volcanic cycle will give rise to sheet flows followed by pillow flows. The cause of these temporal variations in the magma supply is unknown but may be related to a renewed phase of mantle melting. The magma chamber beneath the ridge segment between the CFZ and the 11°45′N OSCs is thought to be in a stage of contraction. This is expressed by the recent emplacement of glassy pillow flows along the crest of the ridge at 10°41.5′N and 11°15′N, by the general lack of high-temperature hydrothermal activity along this ridge segment, and by the disruption or absence of

a magma-chamber reflection (indicating a low magma budget) south of 11°N and beneath the western ridge segment of the 11°45'N OSCs.

Macdonald *et al.* (1984, 1986) have proposed that two separate magma chambers feed the opposing ridge segments at OSCs, as opposed to a single, wide magma chamber shared between the overlapping rifts as suggested by Lonsdale (1983, 1985a,b). Seismic-reflection profiles across the overlap basins of the OSCs at 9°03'N and 11°45'N do not reveal a magma-chamber reflection, and profiles across smaller OSCs at 12°37'N and 12°54'N show gaps in the axial magma-chamber reflection (Avedik & Geli 1987, Detrick *et al.* 1987). Analyses of basalt dredged from OSCs between 5°30'N and 14°30'N along the EPR show that the opposing ridge tips of the OSCs have distinct petrologic and geochemical signatures (Thompson *et al.* 1985, Langmuir *et al.* 1986). These geophysical and petrologic observations suggest that the axial magma chamber is disrupted at OSCs, in support of the model of Macdonald *et al.* (1984, 1986). Investigations of OSCs at 9°03'N (Sempere & Macdonald 1986), 11°45'N (Thompson *et al.* 1985), and 12°45'N (Antrim *et al.* 1985, Hékinian *et al.* 1985a) suggest that although there is morphological overlap between the eastern and western ridges, there is no overlap in the active volcanic zones. In these three cases, the northern limb of the overlap system seems to prevail. The association of Unit I flows and their associated collapse structures with older flows on the 11°45'N OSCs supports this interpretation. The Argo and ANGUS data show that active hydrothermal vents and recent sheet flows occur on the eastern ridge segment, whereas the western ridge segment is dominated by older Unit II and III flows (Fig. 3). These observations support Macdonald *et al.* (1984, 1986, 1988) and Sempere & Macdonald's (1986) contention that the geometry of OSCs is transient in that one or both OSCs tips can propagate along the ridge axis. Collapse structures south of 11°46'N on the eastern ridge segment are much narrower than those between 11°46'N and 11°53'N (Fig. 10). This difference suggests that the magma chamber beneath the zone of weakness is propagating southward, producing uplift of old oceanic basement (Unit III terrane), parts of which collapse along fractures. The lows are then filled with fresh volcanic flows and are sites of hydrothermal activity. The striking similarity of the 11°45'N OSCs (Fig. 3) with the 9°03'N OSCs (Sempere & Macdonald 1986) supports the evolutionary model for the occurrence and evolution of OSCs proposed by Macdonald *et al.* (1984, 1986, 1988).

Conclusions

The along-strike variations in lava-flow type and age along the EPR north of the CFZ from 10°19'N to 11°53'N are similar to those observed by Francheteau & Ballard (1983) in spatially limited investigations of the EPR between 13°N and 21°N. However, our extensive bottom coverage has shown that young volcanic flows have a patchy distribution. Although the presence of a shallow crustal magma chamber at active mid-ocean ridges is a fundamental parameter in the formation of oceanic crust, the shape, longevity, along-strike variability, and dynamic behavior of axial magma chambers are the subject of controversy (Lonsdale 1986, Macdonald *et al.* 1986, Detrick *et al.* 1987). Seismic, morphologic, and petrologic data suggest that a narrow (<4–6 km wide) magma chamber underlies the ridge axis and is continuous for several tens of km along-axis (Detrick *et al.* 1987). Where the magma budget is low, such as at the study area north of the CFZ, and the axial magma chamber is relatively small, incompletely mixed, and disrupted by OSCs (Macdonald *et al.* 1986, Detrick *et al.* 1987), lavas will be geochemically and petrologically diverse (Thompson *et al.* 1985, Langmuir *et al.* 1986), and the most recent volcanic flows will have a more patchy distribution than in areas where the magma budget is high.

Acknowledgements

The 1984 ANGUS phase of this investigation was supported by the National Science Foundation, Grant No. OCE 83-09977; the Argo 1985 program was funded by the Office of Naval Research, Geology and Geophysics Contract No. N00014-82-C-0743 and the Secretary of the Navy Chair in Oceanography, Contract No. N00014-85-G-0242. Participation of French scientists in the Argo 1985 program was made possible by IFREMER and CNRS/PIROCEAN. Any use of trade names is for descriptive purposes only and does not imply endorsement by the U.S. Geological Survey. We are indebted to the engineers of the Deep Submergence Laboratory, Woods Hole Oceanographic Institution, who kept ANGUS and Argo operational at sea. Patricia Forrestal prepared all of the illustrations. We thank Joe Cann, Kim Klitgord, and Hans Schouten for their helpful discussions and suggestions during the preparation of this report, and K. C. Macdonald, E. E. Davis, and T. J. Barrett for their helpful reviews of the manuscript. This is contribution No. 6497 of the Woods Hole Oceanographic Institution.

References

Anderson, R.N. & Noltimier, H.C. (1973): A model for the horst and graben structure of mid-ocean ridge crests based upon spreading velocity and basalt delivery to the oceanic crust. *Geophys. J. Roy. Astron. Soc.* **34**, 137-147.

ANTRIM, L.K., SEMPERE, J.C. & MACDONALD, K.C. (1985): High resolution study of overlapping spreading centers on the East Pacific Rise near 13°N. *EOS, Trans. Amer. Geophys. Union* **66**, 969.

AVEDIK, F. & GELI, L. (1987): Single-channel seismic reflection data from the East Pacific Rise axis between latitude 11°50'N and 12°54'N. *Geology* **15**, 857-860.

BALLARD, R.D. (1980): Mapping the mid-ocean ridge. *Proc. 12th Ann. Meet., Offshore Tech. Conf.* **1**, 55-64.

_____ & FRANCHETEAU, J. (1982): The relationship between active sulfide deposition and axial processes of the mid-ocean ridge. *Mar. Tech. Soc. J.* **16**, 8-22.

_____ & _____ (1983): Geologic processes of the mid-ocean ridge and their relation to sulfide deposition. *In* Hydrothermal Processes at Seafloor Spreading Centers (P.A. Rona, K. Bostrom, L. Laubier & K.L. Smith, Jr., eds.). Plenum Press, New York, 17-25.

_____, _____, JUTEAU, T., RANGIN, C. & NORMARK, W.R. (1981): East Pacific Rise at 21°N: the volcanic, tectonic and hydrothermal processes of the central axis. *Earth Planet. Sci. Lett.* **55**, 1-10.

_____, HÉKINIAN, R. & FRANCHETEAU, J. (1983): Geological setting of hydrothermal activity at 12°50'N on the East Pacific Rise: submersible study. *Earth Planet. Sci. Lett.* **69**, 176-186.

_____, HOLCOMB, R.T. & VAN ANDEL, T.H. (1979): Galapagos Rift at 86°W, 3. Sheet flows, collapse pits, and lava lakes of the rift valley. *J. Geophys. Res.* **84**, 5407-5422.

_____, VAN ANDEL, T.H. & HOLCOMB, R.T. (1982): The Galapagos rift zone at 86°W, 5. Variations in volcanism, structure and hydrothermal activity along a 30-kilometer segment of the rift valley. *J. Geophys. Res.* **87**, 1149-1161.

BRATT, S.R. & SOLOMON, S.C. (1984): Compressional and shear wave structure of the East Pacific Rise at 11°20'N: Constraints from three-component ocean bottom seismometer data. *J. Geophys. Res.* **89**, 6095-6110.

CRANE, K. (1985): The spacing of rift axis highs: dependence upon diapiric processes in the underlying asthenosphere. *Earth Planet. Sci. Lett.* **72**, 405-415.

DEFFEYES, K.S. (1970): The axial valley: a steady state feature in the terrain. *In* Megatectonics of Continents and Oceans (H. Johnson & B.C. Smith, eds.). Rutgers Univ. Press, Brunswick, N.J., 194-222.

DETRICK, R.S., BUHL, P., VERA, E., MUTTER, J., ORCUTT, J., MADSEN, J. & BROCHER, T. (1987): Multichannel seismic images of an axial magma chamber along the East Pacific Rise between 9° and 13°N. *Nature* **326**, 35-41.

FRANCHETEAU, J. & BALLARD, R.D. (1983): The East Pacific Rise near 21°N, 13°N, and 20°S: inferences for along-strike variability of axial processes of the mid-ocean ridge. *Earth Planet. Sci. Lett.* **64**, 93-116.

_____, JUTEAU, T. & RANGIN, C. (1979): Basaltic pillars in collapsed lava ponds on the deep ocean floor. *Nature* **281**, 209-211.

HARRIS, S.E. & BALLARD, R.D. (1986): ARGO: Capabilities for deep ocean exploration. *Proc. Oceans '86, Mar. Tech. Soc.*, Washington, D.C., **1**, 1-6.

HÉKINIAN, R., AUZENDE, J.M., FRANCHETEAU, J., GENTE, P., RYAN, W.B.F. & KAPPEL, E.S. (1985a): Offset spreading centers near 12°53'N on the East Pacific Rise: Submersible observations and composition of the volcanics. *Mar. Geophys. Res.* **7**, 359-377.

_____, FRANCHETEAU, J. & BALLARD, R.D. (1985b): Structural evolution of hydrothermal deposits at the axis of the East Pacific Rise. *Oceanol. Acta* **8**, 1-9.

KLITGORD, K.D. & MAMMERICKX, J. (1982): Northern East Pacific Rise: Magnetic anomaly and bathymetric framework. *J. Geophys. Res.* **87**, 6725-6750.

LALOU, C., BRICHET, E. & HÉKINIAN, R. (1985): Age data of sulfide deposits from axial and off-axial structures on the East Pacific Rise near 12°50'N. *Earth Planet. Sci. Lett.* **75**, 59-71.

LANGMUIR, C.H., BENDER, J.F. & BATIZA, R. (1986): Petrologic and tectonic segmentation of the East Pacific Rise, 5°30'-14°30'N. *Nature* **322**, 422-429.

LONSDALE, P. (1977): Structural geomorphology of a fast-spreading rise crest: The East Pacific Rise near 3°25'S. *Mar. Geophys. Res.* **3**, 251-293.

_____ (1983): Overlapping rift zones at the 5.5°S offset of the East Pacific Rise. *J. Geophys. Res.* **88**, 9393-9406.

_____ (1985a): Nontransform offsets of the Pacific-Cocos plate boundary and their traces on the rise flank. *Geol. Soc. Amer. Bull.* **96**, 313-327.

_____ (1985b): Linear volcanoes along the Pacific-Cocos plate boundary, 9°N to the Galapagos triple junction. *Tectonophys.* **116**, 255-279.

_____ (1986): Comments on "East Pacific Rise from Siqueiros to Orozco Fracture Zones: Along-strike continuity of axial neovolcanic zone and structure and evolution of overlapping spreading centers" by K. Macdonald, J. Sempere and P.J. Fox. *J. Geophys. Res.* **91**, 10493-10499.

MACDONALD, K.C. (1982): Mid-ocean ridges: fine scale tectonic, volcanic and hydrothermal processes within

the plate boundary zone. *Ann. Rev. Earth Planet. Sci.* **10,** 155-190.

_____ & FOX, P.J. (1983): Overlapping spreading centers: a new kind of accretionary geometry on the East Pacific Rise. *Nature* **302,** 55-58.

_____, SEMPERE, J.C. & FOX, P.J. (1984): East Pacific Rise from Siqueiros to Orozco fracture zones: Along-strike continuity of axial Neovolcanic Zone and structure and evolution of overlapping spreading centers. *J. Geophys. Res.* **89,** 6049-6069.

_____, _____ & _____ (1986): Reply: The debate concerning overlapping spreading centers and mid-ocean ridge processes. *J. Geophys. Res.* **91,** 10501-10511.

_____, _____, _____ & TYCE, R. (1988): Tectonic evolution of ridge axis discontinuities by the meeting, linking or self-decapitation of neighboring ridge segments. *Geology* **15,** 993-997.

MCCONACHY, T., MOTTL, M.J., BALLARD, R.D. & VON HERZEN, R.P. (1986): Geological form and setting of a hydrothermal vent field at 10°56'N, East Pacific Rise: A detailed study using ANGUS and ALVIN. *Geology* **4,** 295-298.

ROSENDAHL, B.R., HÉKINIAN, R. *et al.* (1980): *Initial Reports of the Deep Sea Drilling Project* **54.** U.S. Gov. Printing Office, Washington, D.C., 957 p.

SCHOUTEN, H., KLITGORD, K.D. & WHITEHEAD, J.A. (1985): Segmentation of mid-ocean ridges. *Nature* **317,** 225-229.

SEMPERE, J.C. & MACDONALD, K.C. (1986): Deep-Tow studies of the overlapping spreading centers at 9°03' N on the East Pacific Rise. *Tectonics* **5,** 881-900.

SLEEP, N.H. (1969): Sensitivity of heat flow and gravity to the mechanics of seafloor spreading. *J. Geophys. Res.* **74,** 542-549.

_____ (1975): Formation of ocean crust: Some thermal constraints. *J. Geophys. Res.* **80,** 4037-4042.

THOMPSON, G., BRYAN, W.B., BALLARD, R.D., HAMURO, K. & MELSON, W.G. (1985): Axial processes along a segment of the East Pacific Rise, 10°–12°N. *Nature* **318,** 429-433.

VAN ANDEL, T.H. & BALLARD, R.D. (1979): The Galapagos Rift zone at 86°W, 2. Volcanism, structure and evolution of the rift valley. *J. Geophys. Res.* **84,** 5390-5406.

VAN DOVER, C.L., FRANKS, P.J.S. & BALLARD, R.D. (1987): Prediction of hydrothermal vent locations from distributions of brachyuran crabs. *Limnol. Oceanogr.* **32,** 1006-1010.

VOGT, P.R. (1976): Plumes, subaxial pipe flow, and topography along the mid-ocean ridge. *Earth Planet. Sci. Lett.* **29,** 309-325.

Received June 25, 1987; revised manuscript accepted March 25, 1988.